Mantle wedge control on back-arc crustal accretion

Fernando Martinez* **& Brian Taylor†**

** Hawaii Institute of Geophysics and Planetology, † Department of Geology and Geophysics, School of Ocean and Earth Science and Technology, University of Hawaii at Manoa, Honolulu, Hawaii 96822, USA*

At mid-ocean ridges, plate separation leads to upward advection and pressure-release partial melting of fertile mantle material; the melt is then extracted to the spreading centre and the residual depleted mantle flows horizontally away[1]. In back-arc basins, the subducting slab is an important control on the pattern of mantle advection and melt extraction, as well as on compositional and fluid gradients[2]. Modelling studies[3] predict significant mantle wedge effects on back-arc spreading processes. Here we show that various spreading centres in the Lau back-arc basin exhibit enhanced, diminished or normal magma supply, which correlates with distance from the arc volcanic front but not with spreading rate. To explain this correlation we propose that depleted upper-mantle material, generated by melt extraction in the mantle wedge, is overturned and re-introduced beneath the back-arc basin by subduction-induced corner flow. The spreading centres experience enhanced melt delivery near the volcanic front, diminished melting within the overturned depleted mantle farther from the corner and normal melting conditions in undepleted mantle farther away. Our model explains fundamental differences in crustal accretion variables between back-arc and mid-ocean settings.

The simple geometry of the subducted slab beneath the Lau basin[4] (Fig. 1) and well-constrained spreading-centre kinematics[5], together with our bathymetry and gravity compilation and previous geochemical[6–8] and seismic[9–11] studies, allow a comprehensive study of back-arc crustal accretion variables. We focus on the central and east Lau spreading centres (CLSC and ELSC, respectively) and the southern segments of the latter, termed the Valu Fa ridge (VFR). We refer to them here as the Lau spreading centres, although other spreading axes and rifts have been identified in the northern basin[5,12] (Fig. 1). Figure 2 summarizes the characteristics of the Lau spreading centres, including their cross-sectional area or 'inflation', which is a measure of their magmatic robustness[13] (see Supplementary Information). Basin-wide gridded gravity and bathymetry data were used to calculate the mantle Bouguer anomaly, and to remove the across-basin gradient due to slab and subduction effects (see Supplementary Information). Unlike the situation at mid-ocean ridges, this adjusted mantle Bouguer anomaly forms relative axial maxima[14]. The origin and magnitude of the relative maxima of this adjusted anomaly correlates with other parameters (depth, morphology, crustal structure and composition) that define distinct zones of crustal accretion (Fig. 2). We describe each zone in turn before presenting a model to explain the observations.

Zone 1 in Fig. 2 has been interpreted[15] as a rifted and volcanic terrain representing crust that pre-dated the establishment of the present spreading systems. As the basin opened, the ridge system that evolved into the VFR and ELSC originated in the northern basin near the arc volcanic front and propagated asymmetrically southward into this terrain, preferentially rifting into the crust near the volcanic front, as occurs at other back-arc basins[16,17]. Crustal accretion on these axes, however, was roughly symmetric so that with time the spreading centres separated from the volcanic front.

Located at the southern end of the spreading system and closest (40–60 km) to the volcanic front, the VFR has a narrow triangular axial high that is more peaked than typical mid-ocean-ridge axial highs[18]. This shape has been attributed to the more viscous nature—compared to mid-ocean-ridge basalt (MORB)—of the basaltic andesite to rhyodacitic composition of the erupted lavas[18], which have affinities to the proximal volcanic arc[7,8]. The VFR is the shallowest part of the spreading axes, and has high inflation (1–6 km^2) and low values of adjusted mantle Bouguer anomaly (Fig. 2). An axial magma chamber reflector has been imaged almost continuously south of 20° 30′ S (ref. 9), and active hydrothermal vent fields[19] occur south of 21° 50′ S. Seismic refraction lines[10,11] indicate that zone 2 crustal thicknesses are 7.5–9 km, significantly thicker than at typical mid-ocean ridges, both near the VFR axis at 22°–22° 30′ S and west of the CLSC at 18° 25′ S. Zone 2 represents crust that was generated when the spreading centre was near the volcanic front and in a magmatically robust stage, analogous to the present-day VFR. This terrain displays abyssal-hill-like morphology in a few places, but much more often shows a hummocky texture with numerous crescent-shaped highs that are concave toward the axis in plan view. This landform is characteristic of enhanced ridge volcanism forming small split volcanoes[20], and its prevalence throughout zone 2 implies a terrain dominated by volcanic extrusion. Although the sampled portions of the VFR show strong arc affinities[7,8], drilling in a small basin (ODP Site 836) and dredging of a nearby high show both arc- and MORB-like compositions in close proximity within this terrain[15]. Zone 2 sea floor away from the propagation boundary with zone 1 maintains shallow depths off-axis, displays low adjusted mantle Bouguer anomalies (Fig. 2), and has 7.5–9-km-thick crust[10,11]. All of these characteristics evince a robust magmatic state on the VFR and within zone 2, even though the VFR has the lowest spreading rates (~40–60 mm yr^{-1}) of the Lau spreading centres (Fig. 2c).

The ELSC north of the VFR deepens from ~2,000 to ~3,000 m

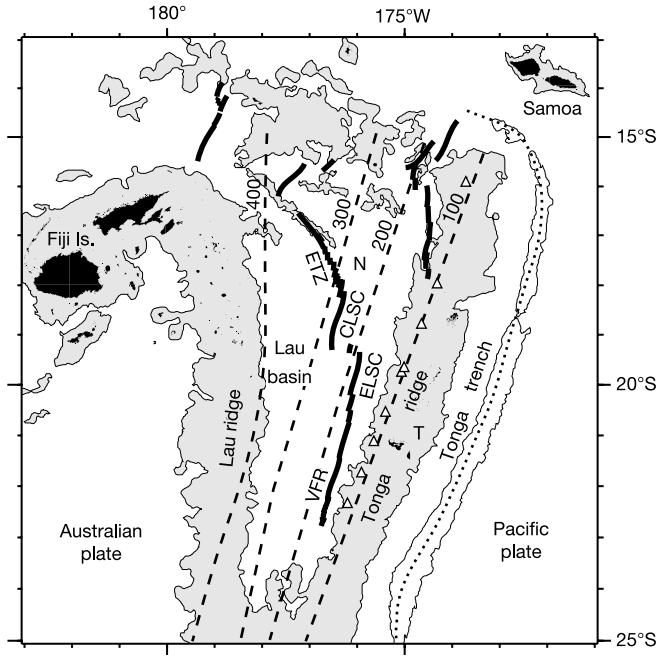

Figure 1 Location map of the Lau basin showing the back-arc spreading centres (heavy lines), trench axis (dotted line) and contours of the subducted slab (dashed lines) labelled in km. The area inside the 2,000-m bathymetry contour is shaded grey, and highlights the Lau and Tonga ridges. The 7,000-m contour surrounds the axis of the Tonga trench. Arc volcanoes are shown as open triangles. Beneath the Lau spreading centres the slab is approximately planar, strikes parallel to the volcanic front, and dips at about 45°. N, Niuafo'ou plate; T, Tonga plate; VFR, Valu Fa ridge; ELSC, east Lau spreading centre; CLSC, central Lau spreading centre; ETZ, extensional transform zone.

and develops a negative cross-sectional area (axial region deeper than flanks) as spreading rates increase from ~60 to ~95 mm yr^{-1} and separation from the volcanic front increases from 60 to 110 km (Fig. 2). Adjusted mantle Bouguer anomalies increase northward by >30 mGal from the relative axial minimum at the 22° 13′ S overlapping spreading centres on the VFR, indicating thinning crust and/or increasing density. Some northward increase in crustal density is likely as compositions change from typical andesites on the VFR to basalts on the ELSC[6,7], but isostatic calculations indicate that a very large density increase (for example, from 2,550 to 2,880 kg m^{-3}) would be required to achieve this deepening without some crustal thinning. As discussed below, this is unlikely given the porosity and Fe content of northern ELSC lavas[6]. Despite fast spreading rates, an axial and across-axis seismic survey[9] did not image a magma chamber reflector north of 20° 30′ S (Fig. 2). Geochemical analysis of rocks dredged from the ELSC[6] indicate a strongly depleted character relative to MORB and decreased arc geochemical signature relative to the VFR. The ELSC ends in a 65-km-wide non-transform offset from the CLSC that encompasses extinct ELSC spreading segments to the north that we infer were also formed by magma deficient spreading before they failed as the CLSC propagated southward. A refraction profile at 18° 33′ S reveals 5.5-km-thick crust at these extinct segments[11]. Zone 3 crust flanks the northern ESLC (Fig. 2) and is characterized by high adjusted mantle Bouguer anomalies, sea floor more than 1 km deeper, and crust 2–3.5 km thinner, than in zone 2. The sea-floor morphology is dominated by low-relief linear abyssal hills, in marked contrast to the more volcanic morphology of zone 2. Although seismically

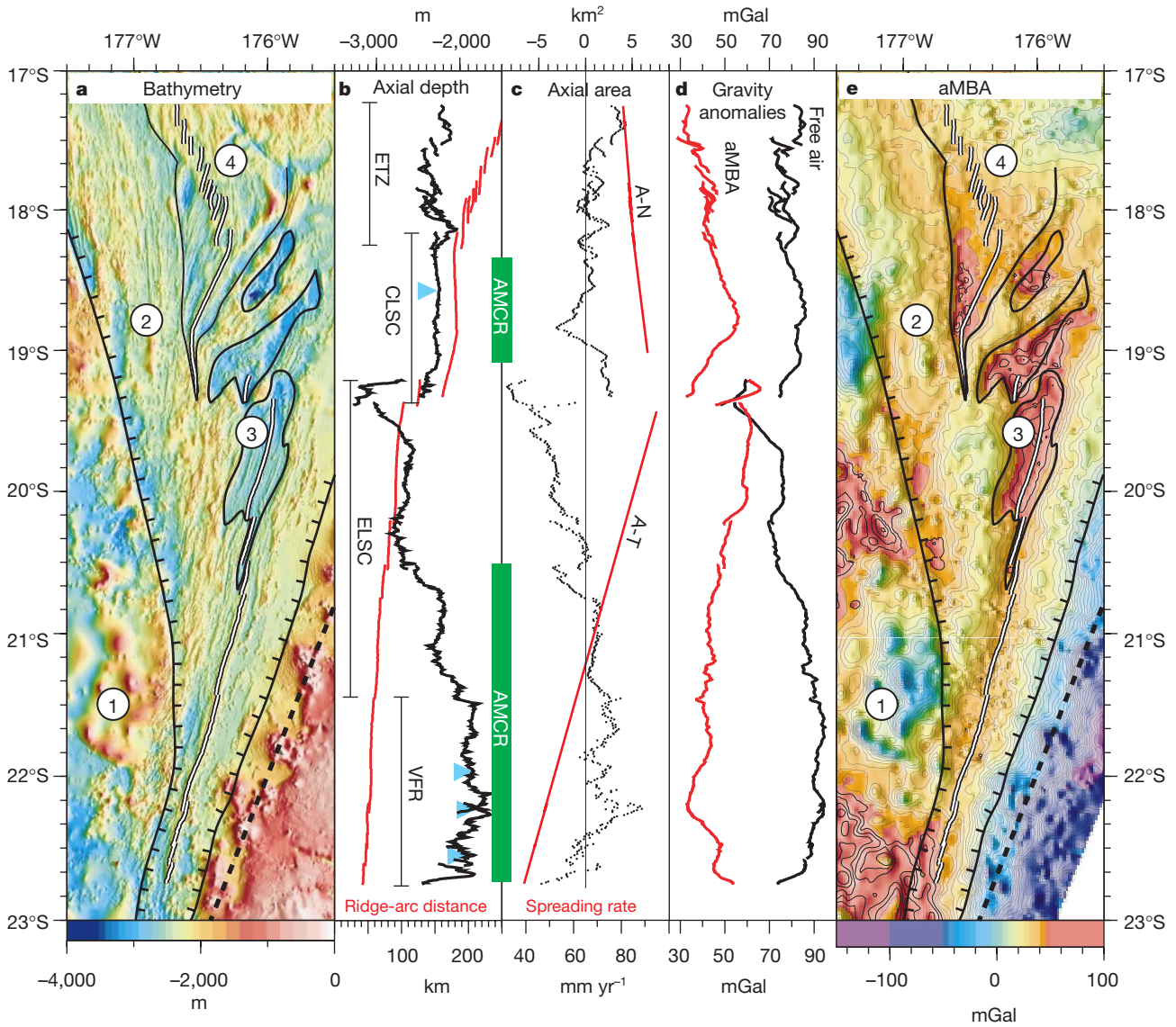

Figure 2 Map and axial profiles of the Lau spreading centres. **a**, Map view of the bathymetry. **b**, Along-axis depth profile (black line) and distance of the spreading centres from the volcanic front (red line). Green areas labelled AMCR indicate where axial magma chamber reflectors have been observed[9]. Blue triangles show active hydrothermal sites[19,21]. **c**, Across-axis area (dots) and spreading rate variation[5] (red line). A–T, Australia–Tonga spreading rates. A–N, Australia–Niuafo'ou spreading rates. **d**, Adjusted mantle Bouguer anomaly (aMBA; red line) and free-air anomaly (black line). The adjusted mantle Bouguer anomaly is the gravity field remaining after the effects of bathymetry, of a 6-km-thick oceanic crustal model, and the long-wavelength gravity gradient due to the slab (see Supplementary Information) are removed from the free-air gravity anomaly. **e**, Map view of the adjusted mantle Bouguer anomaly. Warm colours indicate relatively thin crust, and cool colours relatively thick crust. Panels **a** and **e** have a tectonic interpretation showing location of the boundary (ticked line) between the older crust of the basin (1) and various outlined crustal domains (2–4) associated with the Lau spreading centres (white lines). Dashed line indicates arc volcanic front.

determined crustal thicknesses are only available for the extinct spreading segments of the ELSC, the morphology, depth, gravity, geochemistry and absence of an axial magma chamber reflector all consistently indicate that the ELSC has a decreased magma supply relative to the VFR and CLSC despite higher spreading rates.

The CLSC is located 160–185 km from the volcanic front, and 65 km west of the northern ELSC. As a result of a three-plate configuration in the northern Lau basin[5] (Fig. 1), the CLSC has slightly slower spreading rates (90–85 mm yr^{-1}) than the northern ELSC. Nevertheless, the CLSC axis abruptly shallows and forms an axial high (~2,300 m) with low axial depth variations (Fig. 2). Lavas from the CLSC have MORB-like geochemistry without the depleted character and arc geochemical signal evident in the ELSC[6]. North of its propagating tip, the CLSC has positive inflation, adjusted mantle Bouguer anomalies are ~20 mGal lower than the northern ELSC (Fig. 2), a bright, shallow, axial magma chamber reflector is observed from 18° 21′ S–19° 05′ S (ref. 9), and active hydrothermal vents[21] occur at 18° 36′ S. Relative to the CLSC, the ELSC lavas have lower or equal Fe contents (for example, 9 ± 1% FeO at 8% MgO) and have higher porosity[6]. This indicates that the shallower depth and lower adjusted mantle Bouguer anomalies on the CLSC are not due to crustal compositional (density) differences, but rather to thinner crust on the ELSC. Zone 4 crust formed as the CLSC propagated south, producing variable depths and high gravity anomalies along its pseudofaults. Depths, flank subsidence with age, and gravity anomalies away from the pseudofaults are consistent with normal (6–7 km) oceanic crustal thicknesses. Seismic refraction data confirm that crust formed at the CLSC at 18° 30′ S is 7 km thick[11]. Thus the axis and flanking crust of the CLSC has geophysical, morphologic, seismic, geochemical and hydrothermal characteristics similar to fast-spreading mid-ocean ridges.

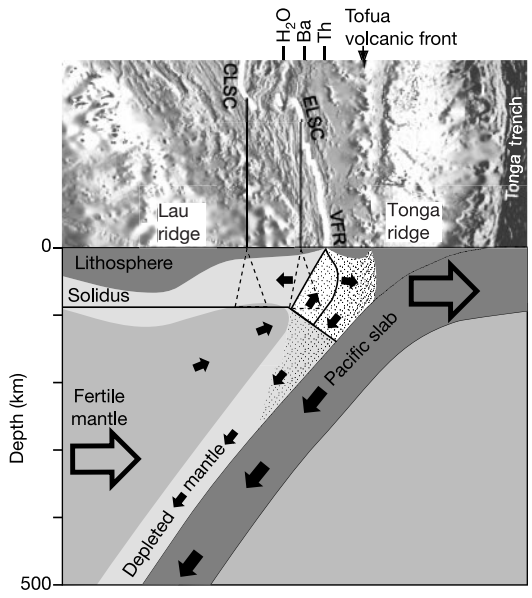

Figure 3 Model of mantle wedge control on back-arc crustal accretion. Upper panel shows an oblique view of the Lau basin bathymetry and spreading centres aligned vertically along the volcanic front, and locates the limits in arc geochemical influence determined from concentrations of H_2O, Ba and Th (ref. 6). The lower panel schematically shows a vertical cut through the mantle wedge at approximately 1:1 scale. Large open arrows indicate the roll-back of the Tonga trench and Pacific slab, and the compensating flow of mantle beneath the Lau basin. Large filled arrows show the subduction component of the Pacific slab, and small solid arrows show flow in the mantle wedge induced by the slab subduction and back-arc spreading. Stippled gradient indicates region of hydrated mantle, with water concentration increasing eastward toward the slab. Within this region, the solidus is shown depressed owing to the effect of water. Region of partial melt in the mantle is shown as the white background beneath stippling. The melting regime of the Valu Fa ridge is shown as the outlined region. It is asymmetric and distorted because of the mantle flow field[3] in the wedge corner. The robust magmatic characteristics of the VFR result from the greater melt production within the hydrated mantle near the corner, and from advection of some arc melts that would otherwise supply the volcanic front. Melt extraction by the spreading centre and by arc volcanism results in a depleted mantle region (light grey). Owing to continuous slab fluid addition, the depleted layer remains weak and can be entrained in the corner flow, become overturned, and re-introduced beneath the back-arc basin. The projected positions of the ELSC and CLSC melting regimes are shown as dashed triangles. The ELSC melting regime is too far from the volcanic front to directly draw significant arc melt. It overlies primarily highly depleted mantle that is being carried into the back-arc by the slab. As a result it produces low amounts of melt, thin crust and deep sea-floor despite fast spreading rates. The projected position of the CLSC melting regime (left dashed triangle) overlies fertile mantle largely removed from slab effects. Consequently the CLSC has crustal thickness, morphology and geochemistry like those of a mid-ocean ridge.

The above observations show that the present-day axes of the Lau basin spreading centres (and the sea floor generated through time on these axes) display characteristics that vary systematically with their position over the mantle wedge—but not with spreading rate. We propose that these variations result from the migration with time of the melt source regions of the back-arc spreading centre through a mantle wedge that is variably melt enhanced/depleted spatially (Fig. 3). A general feature of intra-oceanic arc systems is a gradient in depletion of high-field-strength elements relative to MORB that increases from the back-arc toward the arc volcanic front[22–24]. It has been shown that such a pattern exists even without back-arc spreading[22,23] so that the mantle wedge is self-depleting, probably because water released from the slab lowers the melt solidus[25]. This melt buoyantly rises, underplating, intruding or erupting through the upper plate, or is driven to the volcanic front by subduction-induced flow[26], and leaves a residual mantle depleted of a melt fraction. Corner flow induced by subduction drives the depleted layer toward the wedge corner, where increasing water concentrations from the slab promote additional melting[25] and maintain low viscosity, permitting the otherwise stronger[27,28] depleted layer to continue to flow. At the mantle wedge corner, viscous coupling with the subducting slab overturns the depleted layer and carries it back beneath the back-arc basin (Fig. 3).

When spreading propagates into this depleted and hydrated wedge corner, as at the VFR, its melting regime advects the mantle upward as a consequence of plate separation and causes additional and enhanced melting from this source. It also directly draws to the spreading centre some of the melts that would otherwise contribute to arc volcanic front magmatism[3]. With increasing separation of the spreading centres from the volcanic front, as at the ELSC, the magmatic regimes advect less of the arc volcanic front melt and are increasingly restricted to generating melt solely by advecting the depleted wedge corner. Consequently, as this depleted corner zone is now even more depleted, having had a melt component removed by previous spreading and by volcanic front magmatism, the total amount of melt that can be produced decreases. This results in thinner and deeper crust, low inflation, absence of magma chamber reflectors, high adjusted mantle Bouguer anomalies, and the high geochemical depletion characteristics[6] of the ELSC. Sufficiently far from the wedge corner, however, undepleted mantle must be advecting into the mantle wedge to balance the overall eastward roll-back of the Pacific slab. Such a mantle flow has been inferred on the basis of the recent change in isotopic signature of basin lavas from Pacific to Indian type[29]. The melt source region of the CLSC intersects this undepleted mantle so that the spreading centre has typical mid-ocean-ridge characteristics for its spreading rate. Indeed, we speculate that it was the increasingly more refractory mantle beneath the ELSC (and its increasing viscosity as it separates

from the slab hydration source that permits refractory mantle to flow) that may have promoted the propagation of the CLSC to replace this system.

Spreading in the Lau back-arc basin is at present well-organized, as at mid-ocean ridges[5,12], but, as we have shown, the supply of magma is modulated by mantle wedge compositional controls and arc melt additions. Similar controls are indicated in the Mariana trough, even though the slab there is steeper, and rates of spreading and subduction are slower[30]. In the northern Mariana trough[16], the spreading centre varies from magmatically robust, to magma starved, to normal as it separates from the volcanic front, and in the southern trough the spreading centre changes from an axial valley to an axial high as it approaches the volcanic front[30]. These variations in relative magma supply with proximity to the volcanic front are similar to those we report here for the Lau basin, and support the generality of our model of mantle wedge control on back-arc crustal accretion.

Received 22 October 2001; accepted 14 February 2002.

1. Langmuir, C. H., Klein, E. M. & Plank, T. in *Mantle Flow and Melt Generation at Mid-Ocean Ridges* (eds Phipps Morgan, J., Blackman, D. K. & Sinton, J. M.) (American Geophysical Union, Washington DC, 1992).
2. Davies, J. H. & Stevenson, D. J. Physical model of source region of subduction zone volcanics. *J. Geophys. Res.* **97,** 2037–2070 (1992).
3. Ribe, N. M. Mantle flow induced by back arc spreading. *Geophys. J. Int.* **98,** 85–91 (1989).
4. Chiu, J.-M., Isacks, B. L. & Cardwell, R. K. 3-D configuration of subducted lithosphere in the western Pacific. *Geophys. J. Int.* **106,** 99–111 (1991).
5. Zellmer, K. E. & Taylor, B. A three-plate kinematic model for Lau Basin opening. *Geochem. Geophys. Geosyst.* [online] **2,** 2000GC000106 (2001).
6. Pearce, J. A. *et al.* in *Volcanism Associated with Extension at Consuming Plate Margins* (ed. Smellie, J. L.) 53–75 (Geological Society, London, 1995).
7. Vallier, T. L. *et al.* Subalkaline andesite from Valu Fa Ridge, a back-arc spreading center in southern Lau Basin: petrogenesis, comparative chemistry, and tectonic implications. *Chem. Geol.* **91,** 227–256 (1991).
8. Jenner, G. A., Cawood, P. A., Rautenschlein, M. & White, W. M. Composition of back-arc basin volcanics, Valu Fa ridge, Lau Basin: Evidence for a slab-derived component in their mantle source. *J. Volcanol. Geotherm. Res.* **32,** 209–222 (1987).
9. Harding, A. J., Kent, G. M. & Collins, J. A. Initial results from a multichannel seismic survey of the Lau back-arc basin. *Eos* **81,** F1115 (2000).
10. Turner, I. M., Peirce, C. & Sinha, M. C. Seismic imaging of the axial region of the Valu Fa Ridge, Lau Basin—the accretionary processes of an intermediate back-arc spreading ridge. *Geophys. J. Int.* **138,** 495–519 (1999).
11. Crawford, W. C., Hildebrand, J. A., Dorman, L. M., Webb, S. C. & Wiens, D. A. Tonga Ridge and Lau Basin crustal structure from seismic refraction data. *J. Geophys. Res.* (in the press).
12. Taylor, B., Zellmer, K., Martinez, F. & Goodliffe, A. Sea-floor spreading in the Lau back-arc basin. *Earth Planet. Sci. Lett.* **144,** 35–40 (1996).
13. Scheirer, D. & Macdonald, K. C. Variation in cross-sectional area of the axial ridge along the East Pacific Rise—Evidence for the magmatic budget of a fast spreading center. *J. Geophys. Res.* **98,** 7871–7885 (1993).
14. Sinha, M. C. Segmentation and rift propagation at the Valu Fa ridge, Lau Basin: Evidence from gravity data. *J. Geophys. Res.* **100,** 15025–15043 (1995).
15. Hawkins, J. W. *Backarc Basins: Tectonics and Magmatism* (ed. Taylor, B.) 63–138 (Plenum, New York, 1995).
16. Martinez, F., Fryer, P., Baker, N. A. & Yamazaki, T. Evolution of backarc rifting: Mariana Trough, 20°-24°N. *J. Geophys. Res.* **100,** 3807–3827 (1995).
17. Wright, I. C., Parson, L. M. & Gamble, J. A. Evolution and interaction of migrating cross arc volcanism and back-arc rifting: An example from the southern Havre Trough (35°20′-37°S). *J. Geophys. Res.* **101,** 22071–22086 (1996).
18. Wiedicke, M. & Collier, J. Morphology of the Valu Fa Spreading Ridge in the Southern Lau Basin. *J. Geophys. Res.* **98,** 11769–11782 (1993).
19. Fouquet, Y. *et al.* Hydrothermal activity and metallogenesis in the Lau back-arc basin. *Nature* **349,** 778–781 (1991).
20. Kappel, E. S. & Ryan, W. B. F. Volcanic episodicity and a non-steady state rift valley along northeast Pacific spreading centers: evidence from SeaMARC I. *J. Geophys. Res.* **91,** 13925–13940 (1986).
21. Bortnikov, N. S., Fedorov, D. T. & Murav'ev, K. G. Mineral composition and conditions of the formation of sulfide edifices in the Lau Basin (southwestern sector of the Pacific Ocean). *Geol. Ore Deposits* **35,** 476–488 (1993).
22. Hochstaedter, A. G. *et al.* Across-arc geochemical trends in the Izu-Bonin arc: Constraints on source composition and mantle melting. *J. Geophys. Res.* **105,** 495–512 (2000).
23. Hochstaedter, A. G., Kepezhinskas, P., Defant, M., Drummond, M. & Koloskov, A. Insights into the volcanic arc mantle wedge from magnesian lavas from the Kamchatka arc. *J. Geophys. Res.* **101,** 697–712 (1996).
24. Woodhead, J., Eggins, S. & Gamble, J. High field strength and transition element systematics in island arc and backarc basin basalts: Evidence for multiphase melt extraction and a depleted mantle wedge. *Earth Planet. Sci. Lett.* **114,** 491–504 (1993).
25. Stolper, E. & Newman, S. The role of water in the petrogenesis of Mariana trough magmas. *Earth Planet. Sci. Lett.* **121,** 293–325 (1994).
26. Spiegelman, M. & McKenzie, D. Simple 2-D models for melt extraction at mid-ocean ridges and island arcs. *Earth Planet. Sci. Lett.* **83,** 137–152 (1987).
27. Phipps Morgan, J. The generation of a compositional lithosphere by mid-ocean ridge melting and its effect on subsequent off-axis hotspot upwelling and melting. *Earth Planet. Sci. Lett.* **146,** 213–232 (1997).
28. Hirth, G. & Kohlstedt, D. L. Water in the oceanic upper mantle: implications for rheology, melt extraction and the evolution of the lithosphere. *Earth Planet. Sci. Lett.* **144,** 93–108 (1996).
29. Hergt, J. M. & Hawkesworth, C. J. Pb-, Sr-, and Nd-isotopic evolution of the Lau Basin: Implications for mantle dynamics during backarc opening. *Proc. ODP Sci. Res.* **135,** 505–517 (1994).
30. Martinez, F., Fryer, P. & Becker, N. Geophysical characteristics of the Southern Mariana Trough, 11°50′N-13°40′N. *J. Geophys. Res.* **105,** 16591–16608 (2000).

Supplementary Information accompanies the paper on *Nature's* website (http://www.nature.com).

Acknowledgements

We thank A. Harding, G. Kent and J. Collins for providing gravity and multibeam data from RV *Maurice Ewing* cruise EW9914, and A. Goodliffe and K. Zellmer for providing bathymetric data compilations and for discussions. We also thank D. Scheirer for comments on the manuscript that improved this contribution. This work was supported by the US NSF.

Competing interests statement

The authors declare that they have no competing financial interests.

Correspondence and requests for materials should be addressed to F.M. (e-mail: martinez@soest.hawaii.edu).